STAR Protocols

CellPress
OPEN ACCESS

Protocol

Protocol for quantifying LC3B FRET biosensor activity in living cells using a broad-to-sensitive data analysis pipeline

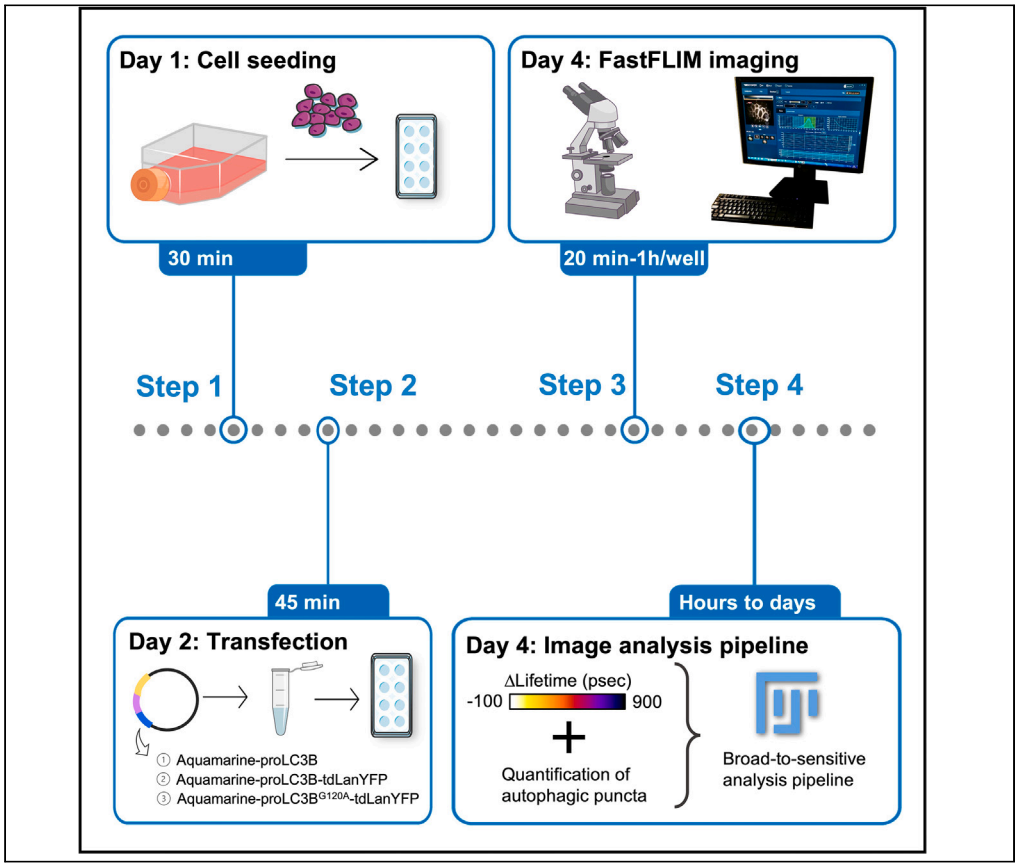

Here, we present a protocol to comprehensively quantify autophagy initiation using the readout of the LC3B Förster's resonance energy transfer (FRET) biosensor. We describe steps for cell seeding, transfection, FRET/FLIM imaging, and image analysis. This protocol can be useful in any physiology- or disease-related paradigm where the LC3B biosensor can be expressed to determine whether autophagy has been initiated or is stalled. The analysis pipeline presented here can be applied to any other genetically-encoded FRET sensor imaged using FRET/FLIM.

Publisher's note: Undertaking any experimental protocol requires adherence to local institutional guidelines for laboratory safety and ethics.

Elif Begüm Gökerküçük, Marc Tramier, Giulia Bertolin

marc.tramier@univ-rennes.fr (M.T.)
giulia.bertolin@univ-rennes.fr (G.B.)

Highlights

Steps for cell seeding, transfection, and FRET/FLIM microscopy with the LC3B biosensor

Extracting raw fluorescence lifetime values and converting them to ΔLifetime format

Quantifying LC3B puncta numbers using steady-state fluorescence intensity images

Histogram, high ΔLifetime, and line analyses to evaluate spatial FRET variations

Gökerküçük et al., STAR Protocols 5, 103181
September 20, 2024
https://doi.org/10.1016/j.xpro.2024.103181

STAR Protocols

CellPress
OPEN ACCESS

Protocol

Protocol for quantifying LC3B FRET biosensor activity in living cells using a broad-to-sensitive data analysis pipeline

Elif Begüm Gökerküçük,[1,2] Marc Tramier,[1,*] and Giulia Bertolin[1,3,*]

[1]Univ Rennes, CNRS, IGDR (Institute of Genetics and Development of Rennes), UMR 6290, F-35000 Rennes, France

[2]Technical contact

[3]Lead contact

*Correspondence: marc.tramier@univ-rennes.fr (M.T.), giulia.bertolin@univ-rennes.fr (G.B.)
https://doi.org/10.1016/j.xpro.2024.103181

SUMMARY

Here, we present a protocol to comprehensively quantify autophagy initiation using the readout of the microtubule associated protein 1 light chain 3 beta (LC3B) Förster's resonance energy transfer (FRET) biosensor. We describe steps for cell seeding, transfection, FRET/FLIM (fluorescence lifetime imaging microscopy) imaging, and image analysis. This protocol can be useful in any physiology- or disease-related paradigm where the LC3B biosensor can be expressed to determine whether autophagy has been initiated or is stalled. The analysis pipeline presented here can be applied to any other genetically encoded FRET sensor imaged using FRET/FLIM.

For complete details on the use and execution of this protocol, please refer to Gökerküçük et al.[1]

BEFORE YOU BEGIN

The LC3B biosensor is a FRET (Förster's resonance energy transfer)-based molecular probe designed to follow ATG4B (autophagy related 4B cysteine peptidase)-dependent regulations of the key autophagy protein MAP1LC3B/LC3B (microtubule associated protein 1 light chain 3 beta) in living cells. A pivotal step in autophagy is the conjugation of LC3B to phosphatidylethanolamine (PE) of the phagophore membrane.[2–4] Prior to this event, inactive LC3B (proLC3B) that has additional five amino acids in its C-terminus needs to be activated.[2,5,6] For LC3B to become functionally active, these five amino acids must be proteolytically cleaved by the cysteine protease ATG4B – a process known as proLC3B priming.[2,5,6] This is essential for the conjugation of LC3B to the phagophore, as this cleavage exposes the critical C-terminal glycine residue (G120) which forms an amide bond with PE.[4,5] While the primed LC3B is referred as LC3B-I, the PE-bound form is referred as LC3B-II. In addition to phagophore membrane conjugation, LC3B has been shown to conjugate other proteins through a post-translational modification process referred as "LC3ylation".[7,8] Recent studies demonstrated that ATG4B can also reverse this process by acting as a deconjugating enzyme to regulate LC3ylation levels.[7,8]

To monitor ATG4B activities on LC3B in living cells, we developed the LC3B biosensor by flanking the N and C termini of proLC3B with a donor-acceptor FRET pair of Aquamarine (donor) and tdLanYFP (acceptor)[9–11] (Figure 1A). When ATG4B is inactive and cannot prime proLC3B within the sensor, FRET occurs between Aquamarine and tdLanYFP. Conversely, the ATG4B priming activity cleaves after residue G120 and separates Aquamarine and tdLanYFP. This results in the loss of FRET. Therefore, the FRET effect enables the real-time monitoring of ATG4B-dependent proLC3B priming. After the loss of C-terminal tdLanYFP, the resulting Aquamarine-LC3B-I is involved in autophagosome formation when it is conjugated to the PE head groups. In this case, the primed biosensor behaves similarly to classical,

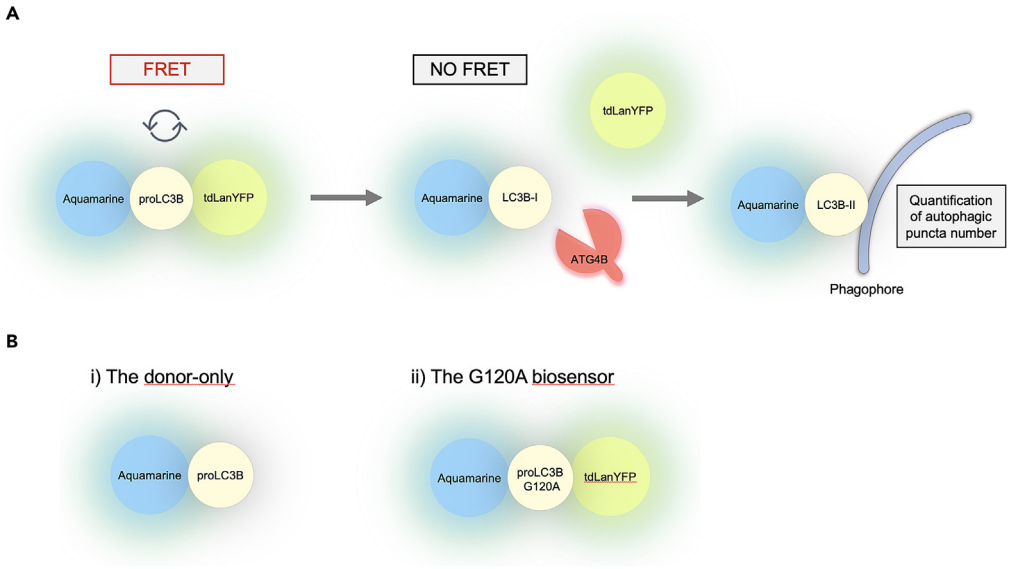

Figure 1. Cartoons showing the LC3B biosensor and the different constructs used in this protocol to extract critical lifetime information

(A) Design and the FRET readout of the LC3B biosensor when expressed in cells.

(B) Design of (i) the donor-only and (ii) the G120A biosensor constructs.

fluorophore-tagged LC3B probes and it forms puncta-like structures. These autophagic puncta can then be quantified to estimate the number of autophagosomes. Of note, in cells where ATG4B is not the main contributor of LC3B priming, other members of the ATG4 family of proteases (ATG4A, C or D) may prime the LC3B biosensor. Therefore, the implementation of the biosensor in such systems should consider the potential involvement of these alternative proteases.

To quantify FRET efficiency within the LC3B biosensor, we use a FastFLIM (fluorescence lifetime imaging microscopy) setup.[12] Although the sensor is fully compatible with conventional ratiometric FRET approaches, FRET quantification by FLIM offers numerous advantages. This includes the accurate determination of FRET efficiency, and the fraction of interacting donor molecules. Lifetime is unaffected by changes in fluorophore concentration, and it shows a superior insensitivity to experimental variations and instrumental factors.[13] Furthermore, with the introduction of non-fitting methodologies, the long acquisition times required to collect enough photons to fit the fluorescence decay has now been reduced to few seconds.[13]

Cell culture, transfection and FRET/FLIM microscopy

Timing: 4 days

1. Start culturing HeLa cells in Dulbecco's modified Eagle's medium (DMEM) supplemented with 10% fetal bovine serum (FBS) and 1% Penicillin-Streptomycin (P/S).
2. Incubate and grow cells at 37°C with 5% CO_2.
3. When the cells reach 70%–80% confluency, aspirate the media and wash the cells with pre-warmed, 1× phosphate buffer saline (PBS).
4. Remove PBS and add 0.05% Trypsin-EDTA to detach the cells.
5. After incubating cells in Trypsin-EDTA for 3 min, neutralize it with at least two volumes of pre-warmed DMEM media containing 10% FBS and 1% P/S.
6. Centrifuge the cells at 800 × *g* for 5 min at 20°C–23°C.
7. Remove the supernatant and resuspend the cells in pre-warmed DMEM containing 10% FBS and 1% P/S.

8. Count the cell number of the suspension, calculate the appropriate number of cells that is necessary to reach 70%–80% confluency on the day of transfection, and seed cells accordingly into the live cell imaging dish of choice (see also key resources table for an example of imaging dish).
9. Incubate the cells until the next day (more than 14 h) to ensure optimal attachment to the imaging support.
10. On the next day, perform cell transfection using a transfection reagent and protocol of choice (see also the key resources table for an example of transfection reagent).
11. Incubate the cells with the transfection mix for 48 h before FRET/FLIM acquisitions.

Note: When working with the LC3B biosensor, it is important to include donor-only and G120A mutant biosensor as additional experimental conditions and plan transfections accordingly (*cf.* step-by-step method details section and Figure 1B).

12. On the day of FRET/FLIM imaging, start incubating cells with the chosen ATG4B inhibitor at the desired concentration and duration.

⚠ CRITICAL: Do not forget to include solvent-control (e.g., dimethyl sulfoxide [DMSO]) for each of the inhibitors used and to be tested on all types of biosensors used, including LC3B biosensor, G120A mutant biosensor and donor-only.

13. Immediately before imaging, briefly wash cells once with pre-warmed, 1× PBS. Then, add phenol red-free Leibovitz's L-15 imaging medium supplemented with 20% FBS and 1% P/S.

⚠ CRITICAL: Do not forget to supplement the imaging medium with the tested inhibitors, to avoid potential washout effects and a subsequent re-activation of the catalytic activity of ATG4.

14. Perform FRET/FLIM imaging as in.[14]

Note: The FastFLIM setup that has been used in this study allows for real-time calculations of the lifetime image to quantify the FRET events.[12] The microscope is composed of a pulsed, white light laser, a spinning disk, and a fast time-gated intensifier in front of a CCD camera and triggered by the laser pulse. Five time-gated images of 2 ns each and with 2 ns trigger delay are acquired. After this step, a pixel-by-pixel calculation of the mean arrival time of the detected photons is calculated. This corresponds to the non-fitted fluorescence lifetime image. The setup also provides steady-state fluorescence intensity images, which can be used to quantify the LC3B-positive puncta-like structures in addition to FRET events.

Note: The laser power and the exposure time should be set to ensure a sufficient photon budget for lifetime calculation, while avoiding phototoxic effects.[14] These effects, which include photobleaching, could alter the donor lifetime and therefore hamper FRET quantification.[15] Depending on the setup used these parameters could differ. Therefore, it is recommended that these parameters are experimentally determined by the end user before proceeding with image analyses.

15. Download and install Fiji software.[16]

KEY RESOURCES TABLE

REAGENT or RESOURCE	SOURCE	IDENTIFIER
Chemicals, peptides, and recombinant proteins		
DMEM	Thermo Fisher Scientific	41966–029
FBS	Eurobio Scientific	CVFSVF00-01

(*Continued on next page*)

Continued		
REAGENT or RESOURCE	SOURCE	IDENTIFIER
P/S	Thermo Fisher Scientific	15140–122
PBS	Euromedex	ET330-A
0.05% trypsin-EDTA	Thermo Fisher Scientific	25300054
Leibovitz's L-15 medium	Thermo Fisher Scientific	21083–027
Lipofectamine 2000	Invitrogen	11668019
NSC 185058	Selleckchem	S6716
Tioconazole	Sigma-Aldrich	03907
DMSO	Sigma-Aldrich	D2438
Experimental models: Cell lines		
HeLa cells	ATCC	CCL-2. In the original publication,[1] the control and *ATG4B* KO cell lines were gift of Robin Kettler, UCL, UK.
Recombinant DNA		
pCMV Aquamarine-proLC3B	Gökerküçük et al.[1]	https://doi.org/10.1080/15548627.2023.2179845
pCMV Aquamarine-proLC3B-tdLanYFP	Gökerküçük et al.[1]	https://doi.org/10.1080/15548627.2023.2179845
pCMV Aquamarine-proLC3B G120A-tdLanYFP	Gökerküçük et al.[1]	https://doi.org/10.1080/15548627.2023.2179845
Software and algorithms		
Fiji	Schindelin et al.[16]	https://fiji.sc/
Prism 9	GraphPad	https://www.graphpad.com/features
Microsoft Excel	Microsoft	https://www.microsoft.com/en-us/microsoft-365/excel
Other		
CELLview cell culture slides for live-cell imaging	Greiner Bio-One	543979
Custom-built FastFLIM setup (microscope and connected devices) controlled by Inscoper Suite solution	Leray et al.[12]	https://www.inscoper.com/fastflim-frap-rennes-france/
Servier Medical Art, provided by Servier, licensed under a Creative Commons Attribution 3.0 unported license	NA	smart.servier.com

MATERIALS AND EQUIPMENT

DMEM supplemented with 10% FBS and 1% P/S	
Reagent	Amount
DMEM	445 mL
FBS	50 mL
P/S	5 mL
Total	**500 mL**
Store at 4°C for up to 3 weeks.	

Phenol red-free Leibovitz's L-15 imaging medium supplemented with 20% FBS and 1% P/S	
Reagent	Amount
Phenol red-free Leibovitz's L-15 imaging medium	79 mL
FBS	20 mL
P/S	1 mL
Total	**100 mL**
Store at 4°C for up to 3 weeks.	

STEP-BY-STEP METHOD DETAILS

Note: In the data analysis pipeline below, we illustrate the steps required to analyze a dataset collected with the FastFLIM microscope, as in.[1] However, the pipeline is dedicated to the analysis of FLIM images, which can also be acquired with any other setup capable of providing steady-state fluorescence intensity and fluorescence lifetime image acquisitions. The pipeline can also be used for datasets of FLIM images addressing alternative biological paradigms. The dataset presented here was collected from live-cell samples treated with two different ATG4B inhibitors: NSC 185058 (NSC) and tioconazole.[17,18] The analysis pipeline consists of broad readouts – mean ΔLifetime and LC3B puncta numbers – and sensitive ones – histogram, high ΔLifetime pixel and line analyses – to spatially resolve the FRET/FLIM and steady-state fluorescence intensity data.

Note: When working with the LC3B biosensor, we use additional constructs namely donor-only and G120A biosensor (Figure 1B). The donor-only is an internal control that lacks the acceptor moiety and therefore cannot perform FRET. The donor-only reports on the lifetime of LC3B-tagged Aquamarine and helps to determine the characteristic lifetime of this probe in every experimental condition tested. On the other hand, G120A mutant biosensor is a probe that is resistant to proteolytic cleavage by ATG4B. Since it cannot be primed by ATG4B, it displays the maximum FRET/FLIM range achievable with the sensor. Throughout the analysis pipeline, the data collected from the cells expressing these additional constructs will be used to determine critical lifetime information such as mean ΔLifetime value or high ΔLifetime threshold value.

Calculating the mean ΔLifetime

Timing: hours to days

As a general starting point, the FRET/FLIM readout of the LC3B biosensor is determined by calculating the mean ΔLifetime value of each individual cell. This is useful to detect major effects on the presence or absence of the ATG4B-mediated priming of the probe.

Note: Prior to calculating ΔLifetime, raw lifetime values should be extracted. The lifetime images acquired using the FastFLIM setup have a stack of five time-gated images to cover the whole fluorescence decay of a fluorescence protein (FP).[12]

1. Extract the raw lifetime values from the image stack in the Fiji software.[14]
   a. Open the lifetime image stack in Fiji.
   b. In *Analyze>Set measurements*, check the *Limit to threshold* option.

   Note: Once this is done, there is no need to re-do it unless you manually uncheck the option.

   c. Generate a region of interest (ROI) by creating a selection around a cell with the *Freehand* tool.
   d. Save the image with the ROI selection to later copy and paste the very same selection for the other analyses.
   e. Threshold the image to get the signal from the ROI with the *Image>Adjust>Threshold* tool while *Dark background* is applied (Figure 2).

   Note: Thresholding is performed manually, on one lifetime image stack at a time. This is necessary as there is no set threshold that can be applied to all images. The aim here is to collect signal across the entire cellular area as shown in Figure 2-optimal thresholding example.

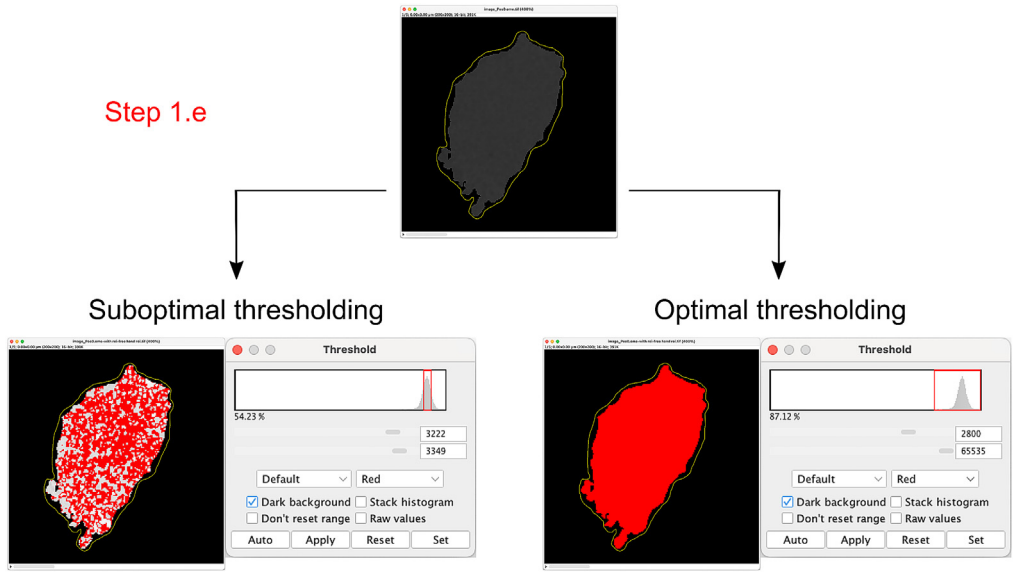

Figure 2. Example of a suboptimal and an optimal thresholding before extracting the raw lifetime values from the lifetime image stack

f. Apply *Image>Stacks>Plot Z-axis Profile* and click on the *List* button to list the five lifetime values corresponding to each of the five images of the stack (Figure 3).
g. Export and average the raw lifetime values of the five lifetime images of the stack.

Note: Once extracted and averaged, this value corresponds to the average lifetime value of all the pixels residing in the thresholded ROI (Figure 3).

⚠ CRITICAL: When thresholding the image, do not click on *Apply*, as this will produce a binary image. Instead, make sure to include all the lifetime-related pixels within the selected area, to isolate them from the background. This step is required if the background values are displayed as 0, instead of being displayed as NaN (Not a Number).

2. Convert the average raw lifetime values into the ΔLifetime format.
   a. Calculate the average mean lifetime value of all the donor-only expressing cells of the control group (i.e., solvent [DMSO] control cells; untreated cells, etc. Hereafter, this value will be referred as the average Aqua-LC3B lifetime) (Figure 3).
   b. Subtract the average lifetime value of a cell (*cf.* step 1.g) from the average Aqua-LC3B lifetime value (*cf.* step 2.a).

Note: This provides a mean ΔLifetime value for each cell expressing the donor-only or the biosensor constructs (Figure 3).

c. Perform statistical analyses to compare the mean ΔLifetime differences between different conditions.

⚠ CRITICAL: When comparing the differences, it is essential to confirm that the type of manipulation – pharmacological or genetical – applied to samples does not cause any perturbation in the donor-only lifetime (*cf.* expected outcomes section and Figures 5A and 5B). This is crucial when testing experimental conditions that may alter the lifetime of Aquamarine by changing the microenvironment of the fluorophore in a FRET-independent manner. Indeed, the fluorescence lifetime of a fluorescent protein (FP) can be

	Cell # 1
Image # 1	3160,6545
Image # 2	3120,4741
Image # 3	3132,6997
Image # 4	3179,1895
Image # 5	3118,8181
Average lifetime (psec)	3142,3672

Step 1.f

Listing the raw lifetime values (psec) of the image stack of cell # 1

Step 1.g

Averaging the raw lifetime values of the five images of the stack

Step 2.a

List the raw lifetime values of all the donor-only expressing cells of the control group

	Cell # 1	Cell # 2	Cell # 3	Cell # 4	Cell # 5	Cell # 6	Cell # 7	Cell # 8	Cell # 9	Cell # 10
Image # 1	3160,6545	3293,1079	3296,74438	3298,1606	3309,6357	3298,6831	3301,9939	3268,7549	3222,347	3288,2014
Image # 2	3120,4741	3292,8838	3297,35522	3285,7444	3296,2007	3282,8665	3316,3164	3247,6609	3396,952	3296,377
Image # 3	3132,6997	3283,543	3296,61597	3292,158	3294,9626	3279,3242	3275,4058	3265,1782	3338,85	3287,2847
Image # 4	3179,1895	3285,5371	3289,3252	3279,8704	3323,1492	3280,5647	3268,042	3269,0396	3316,447	3281,9475
Image # 5	3118,8181	3273,416	3289,78613	3267,7515	3304,4111	3215,2505	3284,7859	3256,5718	3317,9	3297,8542
Average lifetime (psec)	3142,3672	3285,6976	3293,9654	3284,7370	3305,6719	3271,3378	3289,3088	3261,4411	3318,4992	3290,3330

	Cell # 1	Cell # 2	Cell # 3	Cell # 4	Cell # 5	Cell # 6	Cell # 7	Cell # 8	Cell # 9	Cell # 10
Average lifetime (psec)	3142,3672	3285,6976	3293,9654	3284,7370	3305,6719	3271,3378	3289,3088	3261,4411	3318,4992	3290,3330

Calculate the average of all the averages of the control group

Average Aqua-LC3B lifetime = 3274,3359 psec

Step 2.b

ΔLifetime = (Average Aqua-LC3B lifetime) - (Average lifetime)

For cell #1

ΔLifetime = 3274,3359 psec - 3142,3672 psec = 131,9687 psec

Calculate ΔLifetime of each and every cell expressing the donor-only or the biosensor constructs

	Cell # 1	Cell # 2	Cell # 3	Cell # 4	Cell # 5	Cell # 6	Cell # 7	Cell # 8	Cell # 9	Cell # 10
ΔLifetime (psec)	131,969	-11,362	-19,630	-10,401	-31,336	2,998	-14,973	12,895	-44,163	-15,997

Figure 3. Example of raw lifetime values and their conversion into ΔLifetime format

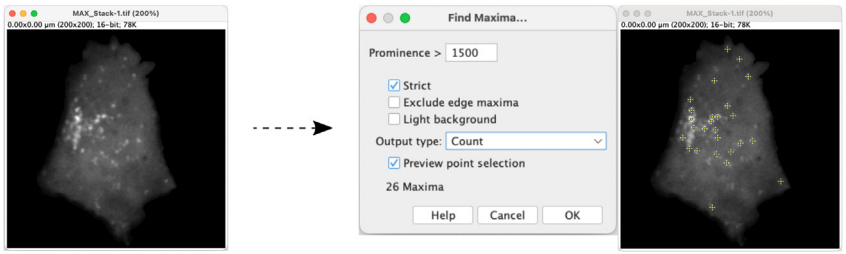

Figure 4. Quantification of the LC3B puncta numbers with the *Process>Find* Maxima function in Fiji

affected by the changes in the temperature, pH, solvent polarity and viscosity, and presence of quenchers in the molecular environment.[19] Moreover, some experimental conditions may involve the overexpression of the protein of interest the FP is tagged to. If the overexpressed protein(s) colocalize or form aggregates, high concentrations of the FP under these conditions can cause self-quenching, which can reduce the fluorescence lifetime.[20–22]

Quantifying the LC3B puncta numbers

Timing: hours to days

Inhibition of ATG4B can lead to a reduced LC3B deconjugation activity which is reflected by the increase in the puncta-shaped structures that represents the autophagosomes and/or LC3ylated proteins.[7,23] With the LC3B biosensor, it is possible to follow the changes in the deconjugation activity by quantifying the number of puncta-shaped structures in the steady-state fluorescence images (Figure 4).

3. Open the steady-state fluorescence intensity image file in Fiji.
4. Copy and paste the same ROI selection that was generated when extracting raw lifetime (*cf.* step 1.c, d).
5. Apply *Clear Outside* to remove signals outside of the ROI.
6. Run *Process>Find Maxima*.
7. In the pop-up menu:
   a. click on Strict and Preview point selection.
   b. select *Output type* as *Count*.
   c. enter a *Prominence* value that can assign each puncta with a point selection.

   Note: This should result in an appearance of a *Maxima* number which reflects the number of puncta-shaped structures. Of note, we use 1500 as a *Prominence* value for our dataset.

8. By applying the same *Prominence* value for each sample, extract and record the *Maxima* numbers for each cell and perform statistical analysis.

Histogram analysis

Timing: hours to days

A complementary, more sensitive approach to the mean ΔLifetime analysis is the histogram analysis.

Note: Mean ΔLifetime analysis reports a single value per cell by calculating the average ΔLifetime across the entire cellular area. Although this method provides an overview of the

overall behavior of the sensor, it may also overlook significant ΔLifetime variations occurring only in specific subcellular areas. Instead, the histogram analysis reports all the ΔLifetime values in a pixel-by-pixel manner. This is performed by extracting the ΔLifetime values of the entire pixel population within a single cell (*cf.* expected outcomes section and Figures 6A, 6B, and 6D). Since each individual pixel is represented in this analysis, the results obtained could be more sensitive to small difference than an average ΔLifetime analysis. This was the case when we explored the effect of knocking down *ATG4B* using siRNAs. While FRET events could be detected thanks to the histogram analyses, they were undetectable using the mean ΔLifetime analysis.[1] By exploring the ΔLifetime values of individual pixels, we gain insights into the spatial heterogeneity of FRET events corresponding to the localized responses of the LC3B biosensor. This approach is particularly valuable in detecting subtle variations, subpopulations of different LC3B forms (proLC3B versus LC3B-I or LC3B-II), or specific cellular regions that may exhibit distinct behaviors or respond to stimuli differently from other areas.

⚠ CRITICAL: Histogram analysis provides a representation of the number of pixels (on the y-axis) with respect to their ΔLifetime value (on the x-axis). It is important to note that this analysis should not be confused with a time-resolved exploration of ΔLifetime changes of a specific pixel.

⚠ CRITICAL: To perform histogram analysis, we should first get a lifetime image with background pixel values displayed as NaN instead of 0. Failure to do so will result in all the background pixels of the lifetime image to have a value of 0, which will be represented in the histogram distribution.

9. Convert the lifetime image with background pixel values displayed as NaN.
   a. Start by applying *Edit>Options>Misc…* and set the *Divide by Zero* option as "NaN".
   b. Open the lifetime image stack in Fiji (hereafter referred as image1).
   c. Duplicate the first image of the stack by following *Image>Duplicate* (hereafter referred as image2).
   d. Threshold image2 to get the signal from the whole cellular area with the *Image>Adjust> Threshold* tool.
      i. Make sure *Dark background* option is not selected and click on *Apply*.

   Note: This will create a binary image where the background pixels display a value of 0, and the cellular areas where threshold was applied will display a value of 255 (hereafter referred as image2a).

   e. Divide image2a by 255 by following *Process>Math>Divide* to set the cellular pixel values as 1 (hereafter referred as image2b).
   f. Divide image1 by image2b by following *Process>Image Calculator.*
      i. On the menu, set *Operation* as *Divide* and select both the *Create new window* and *32-bit (float) result* options.

   Note: This creates a lifetime image stack where the pixels residing in the cellular areas are represented with their original lifetime value, while the background values are represented with NaN.

10. Once the background zero values of the lifetime image stack are converted to NaN, calculate and display the histogram by following the *Analyze>Histogram* function.

⚠ CRITICAL: Here it is important to set a *Bins* value that should consider the characteristics of the data and the preferred level of detail in the resulting histogram. Bins represent intervals or ranges into which data values are grouped. A higher number of bins provides a

more detailed representation of the distribution of data, while a lower number simplifies the histogram. In addition to this, it is also important to set the *X min* and *X max* values based on the data values to include in the histogram. If the entire data range is of interest, setting *X min* to the minimum value and *X max* to the maximum value is appropriate. Alternatively, if focusing on a specific subset of data, *X min* and *X max* can be adjusted to represent only that particular interval.

Note: In the case of the LC3B biosensor, we typically use 1024 as *Bins* value, and set the *X min* and *X max* as 2000 and 4000, respectively. This approach is based on experimental observations wherein the donor-only, wild-type biosensor, and G120A mutant biosensor typically yield raw lifetime values within the range of 2000–4000 picoseconds (psec). By selecting a *Bins* value of 1024, we achieve a granularity of approximately 2 psec between adjacent data points. This choice of binning strategy for the LC3B biosensor allows to maintain an optimal balance between capturing the differences in data distribution with a sufficient sensitivity while avoiding an overwhelming level of intricacy. Nevertheless, we advise the end user to manually optimize these parameters if this protocol is meant to be used with other genetically-encoded FRET sensors.

11. After incorporating parameters, click on the *List* button to display the list of the number of counts per data point.

Note: This list provides the histogram distribution of a cell by displaying the lifetime values in ascending order and showing the number of pixels (counts) per lifetime value.

12. Normalize the pixel counts of each lifetime value with the total sum of pixels.

Note: This can be done by dividing each pixel count per lifetime value by the total number of pixels of that image. This way, the resulting values represent proportions rather than absolute counts.

13. Convert the lifetime data points to ΔLifetime and display on a XY format with their respective pixel proportion values to generate a histogram distribution graph (*cf.* step 2).
14. To add the mode value on the histogram distribution, sort the pixel counts in descending order.

Note: The ΔLifetime data point (bin) with the highest frequency should appear on top of the list and therefore should correspond to your histogram mode value.

High ΔLifetime pixel analysis

Timing: hours to days

A way to derive analytical information from the histogram data is to analyze subset of pixels within a specific range of ΔLifetime values by thresholding.

Note: With the LC3B biosensor, we focus on capturing "high" ΔLifetime pixels as they represent the population of proLC3B pixels that are increasing upon ATG4B inhibition. In other words, high ΔLifetime pixels locate in the sub-cellular areas with significant FRET activity. In these areas, FRET is associated with the population of proLC3B increasing upon ATG4B inhibition in WT biosensor-expressing cells (*cf.* expected outcomes section, Figures 6A and 6E).

⚠ CRITICAL: A critical step here is to be able to select the threshold appropriately. This threshold can be set based on prior knowledge, experimental observations, or statistical considerations enabling the identification of pixels exhibiting significant FRET activity.

The chosen threshold serves as a valuable criterion for subsequent high ΔLifetime pixel analysis to identify specific proportions of proLC3B pixels.

Note: For the LC3B biosensor, we use the mutant G120A biosensor data to determine the threshold. Since the G120A biosensor cannot be proteolytically cleaved by ATG4B, the mean ΔLifetime value of the cells expressing this mutated sensor represents the highest FRET level that can be obtained with the LC3B biosensor. An alternative approach is to use the mean ΔLifetime value of the *ATG4B* knockout (KO) cells expressing the WT biosensor. Since the WT biosensor will only be found as proLC3B in *ATG4* KO cells and without further conversion into LC3B-I or LC3B-II, its mean ΔLifetime values are similar to those of the G120A biosensor.[1]

15. Determine the threshold ΔLifetime value (e.g., G120A biosensor, WT sensor in *ATG4B* KO etc.).
16. Identify the pixels that have ΔLifetime values higher than the threshold and classify them as high ΔLifetime pixels.

Note: This step can be performed on the same list that was previously extracted when performing the histogram analysis (*cf.* step 11).

17. Divide the total number of pixels that are above the threshold ΔLifetime value by the total number of pixels acquired in each image. The resulting ratio represents the proportion of pixels that are classified as "high ΔLifetime pixels".

Line analysis

Timing: hours to days

To visualize the spatial distribution of local variations in ΔLifetime, line analysis can be performed to examine the spatial patterns of FRET events, or the colocalization of these events with specific cellular structures.

18. With the *Straight* tool in Fiji, draw a straight line in a ROI.

Note: To establish the exact position of the line, we advise to use the steady-state fluorescence intensity image, since it allows the identification of puncta-shaped structures therein. It is also important to standardize the length of the line when getting measurements from different ROIs. (*cf.* expected outcomes section, Figure 6A-enlarged images and F).

19. Once the position of the line is determined on the fluorescence image, copy and paste the line to the lifetime image by following *Edit>Selection>Restore Selection.*
20. Select *Analyze>Plot Profile* and click on *List* to extract the lifetime values along the drawn line.
21. Convert the lifetime values into ΔLifetime format by subtracting the average Aqua-LC3B lifetime value from the raw lifetime values along the line.

EXPECTED OUTCOMES

As the LC3B biosensor is expressed ubiquitously in the cells, we typically extract the mean lifetime value of the whole cellular area where all the three forms of LC3B – proLC3B, LC3B-I and LC3B-II – can be found. That is why, the mean lifetime value of a cell expressing the LC3B biosensor represents the lifetime value of the cumulative contribution of all three forms of LC3B. When analyzing the mean ΔLifetime differences, we observed no difference between the ΔLifetime values of donor only-expressing cells treated with NSC or tioconazole, compared to the DMSO condition (Figures 5A and 5B). This confirms that the treatment with either of these inhibitors does not change the lifetime

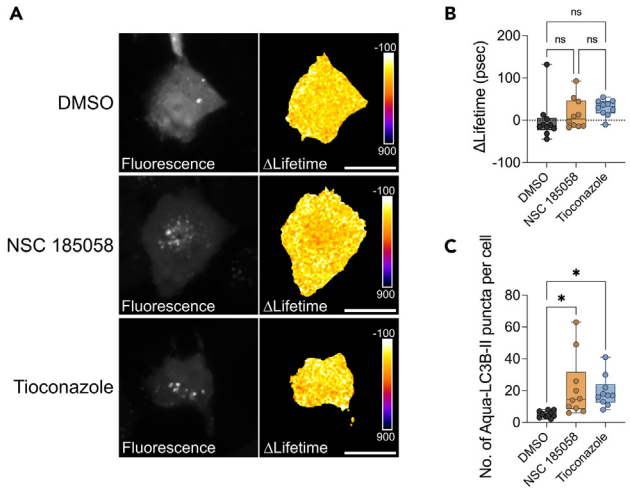

Figure 5. ATG4B inhibition with NSC or Tioconazole does not change the intrinsic Aquamarine mean ΔLifetime, but it alters the Aqua-LC3B-II puncta numbers in HeLa cells expressing the donor-only construct

(A) Representative fluorescence and ΔLifetime images of HeLa cells expressing the donor-only construct and treated with DMSO (6 h), NSC 185058 (6 h, 100 μM) or tioconazole (6 h, 4 μM). Pseudocolor scale: pixel-by-pixel ΔLifetime. Scale bar: 40 μm. Mean ΔLifetime (B) and number of Aqua-LC3B-II puncta (C) analyses of HeLa cells expressing the donor-only construct and treated with DMSO (6 h), NSC 185058 (6 h, 100 μM) or tioconazole (6 h, 4 μM). $n = 10$ cells per condition from one representative experiment (of three) in (B and C). *$p < 0.05$ and ns (not significant) as determined by one-way ANOVA with Tukey's multiple comparison test in (B and C).

properties of the donor-only control probe. Therefore, any change in the lifetime values of biosensor-expressing cells is likely the result of FRET events upon ATG4B inhibition rather than potential intrinsic changes in Aquamarine lifetime.[1] Indeed, when we compare the ΔLifetime differences in biosensor-expressing cells, we observed that the treatment with NSC, but not with tioconazole, significantly increased the ΔLifetime values as compared to the control (Figures 6A and 6B). Altogether, these results provide a first piece of evidence that the proLC3B pool becomes more abundant upon NSC treatment. On the contrary, LC3B-I and LC3B-II pools are still the most abundant forms when cells are treated with tioconazole.

We observed that both the donor-only and the WT biosensor expressing cells reported significantly increased puncta numbers upon NSC or tioconazole treatment as compared to the control (Figures 5A, 5C, 6A, and 6C). In contrast, we observed no difference in cells expressing the priming-defective G120A biosensor with any of the compounds tested (Figures 6A and 6C). The probe remained cytosolic upon ATG4B inhibition and did not display any significant amount of puncta. Overall, these results highlight the previously-reported effect of the ATG4B inhibitors on the deconjugation activity of ATG4B, which can be replicated when using the donor-only and the biosensor constructs.[17]

After the broad analyses of mean ΔLifetime and LC3B puncta numbers, we can proceed with sensitive analyses such as the superposition of the histogram distribution issued from cells in different experimental conditions. With the histogram analysis, we can expect to drive key insights on the FRET status of the biosensors.

- Assessment of the shape and range of the histogram distribution to gain information about the homogeneity or heterogeneity of FRET/FLIM events. A narrow and symmetric histogram distribution suggests a homogeneous FRET population, while a broad or skewed distribution may indicate a heterogeneous mixture of FRET populations or varying environmental conditions affecting FRET efficiency.

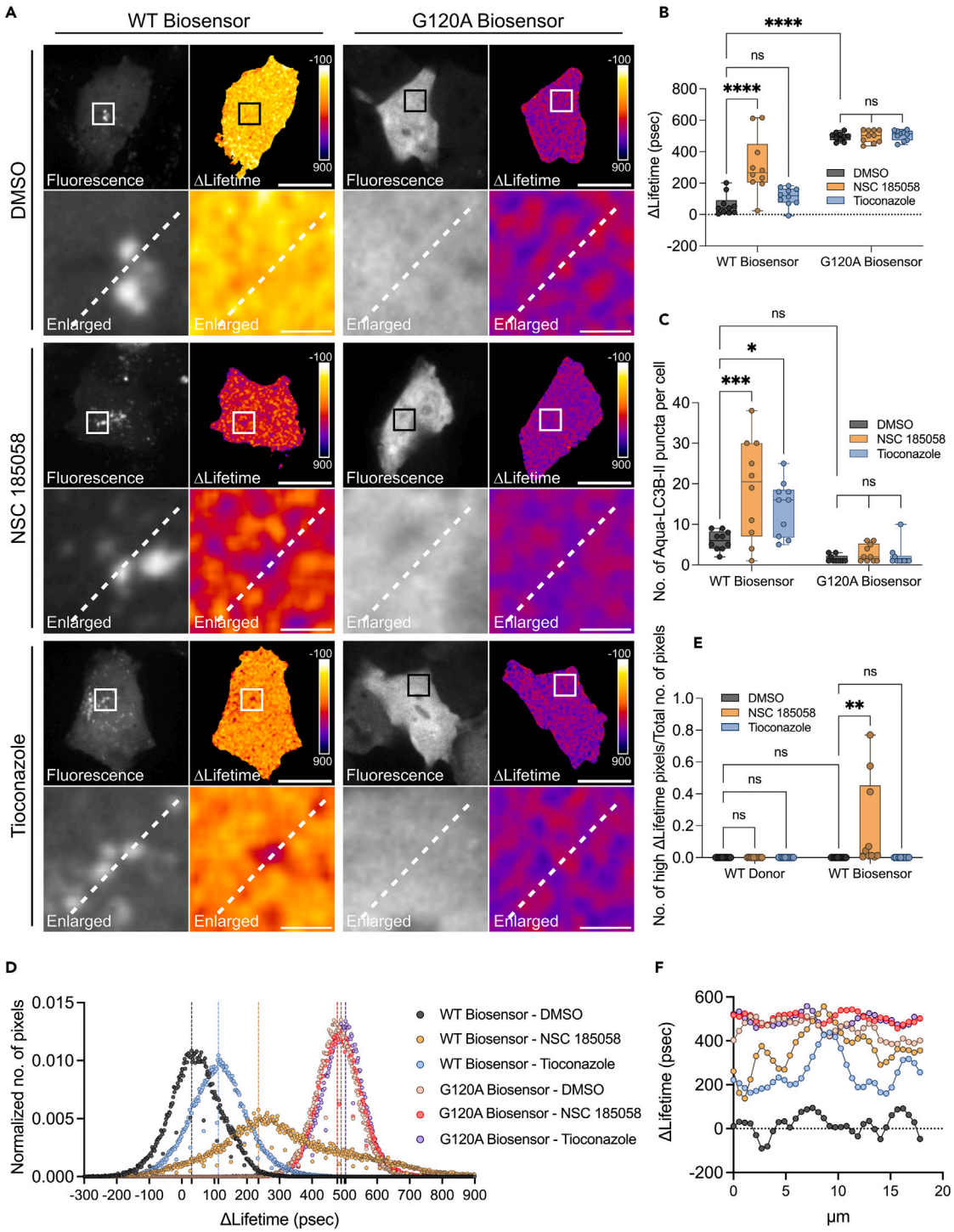

Figure 6. The broad-to-sensitive analysis pipeline applied with the LC3B biosensor quantitatively reports the ATG4B activity in HeLa cells treated with NSC or Tioconazole

(A) Representative fluorescence and ΔLifetime images of HeLa cells expressing the WT or G120A biosensor, treated with DMSO (6 h), NSC 185058 (6 h, 100 μM) or tioconazole (6 h, 4 μM), and analyzed by FRET-FLIM. Squares on the top images of WT or G120A biosensor panels illustrate the location of the enlarged images. Dotted lines on the enlarged images illustrate where the line analysis was performed. Pseudocolor scale: pixel-by-pixel ΔLifetime. Scale bars: overviews, 40 μm; enlarged, 6 μm. Mean ΔLifetime (B), number of Aqua-LC3B-II puncta (C), histogram (D), number of high ΔLifetime pixels (E), and line (F) analysis of HeLa cells expressing the WT or G120A biosensor and treated with DMSO (6 h), NSC 185058 (6 h, 100 μM) or tioconazole (6 h, 4 μM). n = 10 cells per condition from one representative experiment (of three) in (B–E). *$p < 0.05$, **$p < 0.01$, ***$p < 0.001$, ****$p < 0.0001$, ns (not significant) as determined by two-way ANOVA with Tukey's multiple comparison test in (B, C and E).

- Identifying any significant peaks on the histogram distribution that may represent specific FRET/FLIM events. These peaks can provide insights into the presence of distinct molecular interactions or conformational states within the studied system.
- Computation of the statistical measures such as mean, median, mode, and standard deviation to quantify the tendency and variability of the ΔLifetime distribution.
- Performing analytical techniques such as thresholding, segmentation, or classification algorithms to extract specific features or subcellular regions from the image, thus enabling a more detailed analysis and interpretation.
- Identifying outliers or abnormal FRET events which can be indicative of experimental artifacts, noise, or rare FRET events with unique characteristics.

When interpreting histogram distribution of the LC3B biosensor, we assess the changes in the histogram mode values between different conditions. The mode value represents the most frequently occurring ΔLifetime value. Thus, a change in the mode value when compared to the baseline reflects the presence of subpopulations or heterogeneity within the analyzed sample. Indeed, the histogram distributions of the control, tioconazole- or NSC-treated cells expressing the WT biosensor display distinct histogram mode values (Figure 6D). While the control cells exhibited a baseline histogram mode value close to zero (30 psec ΔLifetime), tioconazole- and NSC-treated cells exhibited 112 psec and 235 psec ΔLifetime mode values, respectively. In contrast, the cells expressing the G120A biosensor in all conditions tested exhibited similar histogram mode values that fluctuated around 500 psec of ΔLifetime. These results indicate that the shifts in the histogram mode value observed in the cells treated with the ATG4B inhibitors are specific to the cells that express the WT biosensor, and are likely due to the increase in the proLC3B population.

In addition to histogram analysis, high ΔLifetime analysis can be used to calculate the number of pixels above a certain threshold. As it can be seen in Figure 6E, NSC treatment led to a significant increase in the number of high ΔLifetime pixels compared to the control condition in cells expressing the WT biosensor. This finding was combined with the large histogram mode value shift observed upon NSC treatment and again showing higher ΔLifetime values. Altogether, this indicates that NSC treatment reduces the priming rates of proLC3B, which leads to the accumulation of unprimed, proLC3B. These results also point at NSC as a potent ATG4B inhibitor. On the other hand, tioconazole treatment did not cause a significant increase in the number of high ΔLifetime pixels (Figure 6E). Despite the shift in the histogram mode value compared to that of control cells, the lack of high ΔLifetime pixels suggests that tioconazole is a mild ATG4B inhibitor.

Finally, when assessing the line analysis with the LC3B biosensor, we can expect to follow changes in the microenvironment of the biosensor. Indeed, we observed high ΔLifetime pixels predominantly within or in close proximity of puncta-shaped structures in conditions where ATG4B was genetically downregulated or pharmacologically inhibited. In the latter paradigm, high ΔLifetime pixels with G120A biosensor-like values were prominent in both tioconazole and NSC treated cells (Figure 6F). This spatial distribution of high ΔLifetime pixels underlined their spatial heterogeneity, and their confinement to discrete subcellular regions. Nevertheless, these pixels were only abundant in NSC treated cells as revealed by the high ΔLifetime pixel analysis (Figure 6E), therefore highlighting the importance of performing distinct analyses to fully dissect the differential effects of ATG4B inhibitors.

This analysis pipeline clearly showcases that the implementation of pixel-based statistics allows to determine more accurate and subtle differences in lifetime, which are often lost when relying exclusively on mean ΔLifetime. Moreover, line analyses or alternative approaches to explore the spatial heterogeneity of lifetime further reinforce these differences. Overall, it is advantageous to exploit the spatial information whenever FLIM analyses allow to extract it, and to use it for statistical purposes. This undoubtedly increases the understanding of the mode of action of the biosensor.

LIMITATIONS

Quantification of ATG4B activity with the LC3B biosensor requires the inclusion of the mutant G120A biosensor to establish a robust threshold for calculating the high ΔLifetime values. Alternatively, the lifetime values of the WT biosensor expressed in *ATG4B* KO cells can also be used as a way to establish the amplitude of the FRET response of the biosensor. However, this reliance necessitates the presence of an additional condition throughout the experiments. This poses practical and logistical constraints on the experimental flow. When using the LC3B biosensor in the presence of pharmacological compounds, the G120A condition must also be tested in the presence of each drug. Therefore, this requires extra time and more computer space, and this can be particularly relevant when performing large-scale screenings. If an *ATG4B* KO condition is used as a threshold instead of a G120A mutant, this brings further technical considerations. A potential constraint to be considered is that the KO cell line must be established, validated and systematically used across experiments in addition to control cells. Similarly to G120A, there is the need to use KO and control cells for each single pharmacological compound of interest. Overall, the *ATG4B* KO cell line also comes with additional acquisition analysis times, which can be burdensome when performing large-scale screenings.

By leveraging the distinct characteristic of the mutant biosensor, the presented analysis pipeline achieves enhanced precision in interpreting FRET/FLIM data. Notably, when the analysis pipeline is desired to follow for another FRET biosensor, the availability of a biologically relevant mutant or a suitable control cell line is critical.

The effectiveness of this analysis pipeline relies on the ubiquitous expression and the whole cellular area acquisition of the LC3B biosensor. It is possible to apply this analysis pipeline for any other FRET-based biosensor, although some considerations must be made. If another FRET biosensor exhibits expression patters confined to a sub-cellular location with a limited range of FRET/FLIM dynamics and pixel numbers, the analysis pipeline should be modified to take into account the dynamic range of the FRET response, the overall number of FRET pixels in each experimental condition, and/or adding a specific statistical weight to FRET pixels in a particular subcellular location. In addition, the user should implement an appropriate set of controls relative to the signaling pathway of interest (i.e., loss-of-function mutants, knockouts or knockdown-related conditions, etc.)

It should also be kept in mind that this protocol was optimized on images where the LC3B biosensor was overexpressed in different cell types, such as HeLa or U2OS cells.[1] Although we originally relied on overexpression, our data indicate that the sensor can be used in a variety of cell types. Further, they do not exclude that the same analysis pipeline could be used with LC3B-based FRET vectors expressed at endogenous levels, although this remains to be experimentally validated. In the original study, we also explored the role of members of the ATG4 family on proLC3B cleavage beyond ATG4B.[1] However, it should be experimentally verified whether additional members of the ATG4 or of the ATG8 families participate to the proLC3B-related FRET readout of our probe.

Finally, it should also be noted that the LC3B biosensor has been engineered to perform optimally when coupled with FLIM approaches. Even though rapid FLIM solutions are becoming increasingly accessible within recent commercially-available instrumentation (e.g., STELLARIS 8 FALCON FLIM microscope), the need for specialized equipment and expertise to ensure optimal interpretation of acquired data still remains.

TROUBLESHOOTING

Problem 1

The donor-only lifetime values change significantly between different cells of the same condition (*cf.* step 1).

Potential solution 1

Assuming that the tested ATG4B inhibitors do not cause an intrinsic change in the Aquamarine lifetime, any significant divergence in lifetime values between different cells of the very same condition could indicate the occurrence of photobleaching. Photobleaching can affect the accuracy of FLIM measurements and with this, introduce artifacts in the calculation of the lifetime.[24] To mitigate this issue, imaging parameters should be optimized, such as reducing laser power and minimizing exposure time.

Problem 2

The fluorescence signal of the LC3B biosensor is not detectable in the cytosolic areas (*cf.* before you begin section).

Potential solution 2

When working with the LC3B biosensor, acquiring the signal from the entire cellular area is crucial to be able to apply the analysis pipeline. Due to the variability of the transfection efficiency among cells, it is possible to have cells with different expression levels of the biosensor. This, in turn, results in the lack of signal to be detected especially in cytosolic areas. To overcome this issue, the pixel-by-pixel fluorescence intensity in the first gate can be lowered to 1000 Gy levels. Additionally, transfection conditions including the generation of stable cell lines expressing the biosensor can also be optimized in terms of plasmid amount.

Problem 3

There is a group of pixels with unusual lifetime values outside of the typical range of 2000–4000 psec (*cf.* step 11).

Potential solution 3

The presence of pixels outside the typical lifetime range is a sign of saturation of the fluorescence intensity, which causes distortions in FLIM measurements. These pixels with atypical lifetime values may be the result of mis-trafficked biosensor, potentially due to ectopic expression in cells. Additionally, contamination from background signals or other fluorescence sources such as autofluorescent species can also introduce variations in the canonical lifetime range. Pixels influenced by these factors may display unusual lifetime values, and cells with these pixels should not be included in the analysis.

Problem 4

Even though there is a significant change in mean ΔLifetime values and a substantial shift in the histogram mode value upon treatment, there is no significant difference in the number of high ΔLifetime pixels (*cf.* expected outcomes section).

Potential solution 4

An intermediate case like this is the result of unspecific or sub-optimal FRET events taking place between Aqua-LC3B-II and cleaved tdLanYFP that is in the close vicinity. It is possible that certain compounds, instead of truly inhibiting proLC3B priming, rather promote unspecific FRET events. To be identified as an efficient ATG4B inhibitor, we suggest that a compound should meet all the criteria presented in the broad-to-sensitive pipeline, and display a significant change towards high ΔLifetime values in all the methods of analysis.

Problem 5

The treatment with the inhibitors has no effect or the effect is varying between different experimental replicates (*cf.* before you begin section).

Potential solution 5

Handling inhibitors requires careful attention to ensure accurate and reproducible results. Inhibitors should be stored according to the manufacturer's recommendations, including not only temperature but also light conditions. Freeze-thaw cycles should be avoided, and we recommend using fresh

aliquots for each experiment. Complementary approaches such as western blotting of the various LC3B isoforms should also be performed periodically, to detect any changes on the efficiency of the inhibitors over time.

RESOURCE AVAILABILITY

Lead contact

Further information and requests for resources and reagents should be directed to and will be fulfilled by the lead contact, Giulia Bertolin (giulia.bertolin@univ-rennes.fr).

Technical contact

Further technical and detailed inquiries should be directed to the technical contact, Elif Begüm Gökerküçük (elif-begum.gokerkucuk@pasteur.fr).

Materials availability

Plasmids used in this study are available upon request from the lead contact.

Data and code availability

The source data that support the findings of this study are available upon request from the lead contact. No new code was generated in this protocol.

ACKNOWLEDGMENTS

We thank S. Dutertre and X. Pinson at the Microscopy Rennes Imaging Center (MRic, Biologie, Santé, Innovation Technologique - BIOSIT, Rennes, France) for help and assistance. MRic is member of the national infrastructure France-BioImaging supported by the French National Research Agency (ANR-10-INBS-04). This work was supported by the Centre National de la Recherche Scientifique (CNRS), the University of Rennes, the Ligue Contre le Cancer Comité d'Ille et Vilaine et du Finistere and the Association pour la Recherche sur le Cancer (ARC), and the French National Research Agency (ANR-21-CE11-0002-01) to G.B. and by the Institut National du Cancer (INCa) and ITMO Cancer/Aviesan to M.T. E.B.G. was supported by a fellowship from the Ligue Contre le Cancer and Région Bretagne (Brittany region, France).

AUTHOR CONTRIBUTIONS

E.B.G. designed, performed, and analyzed the experiments and wrote the manuscript. M.T. co-supervised the work, revised the manuscript, and provided funding. G.B. co-supervised the work; designed the experiments; wrote, edited, and revised the manuscript; and provided funding.

DECLARATION OF INTERESTS

The authors declare no competing interest.

REFERENCES

1. Gökerküçük, E.B., Cheron, A., Tramier, M., and Bertolin, G. (2023). The LC3B FRET biosensor monitors the modes of action of ATG4B during autophagy in living cells. Autophagy *19*, 2275–2295. https://doi.org/10.1080/15548627.2023.2179845.

2. Kabeya, Y., Mizushima, N., Ueno, T., Yamamoto, A., Kirisako, T., Noda, T., Kominami, E., Ohsumi, Y., and Yoshimori, T. (2000). LC3, a mammalian homologue of yeast Apg8p, is localized in autophagosome membranes after processing. EMBO J. *19*, 5720–5728. https://doi.org/10.1093/emboj/19.21.5720.

3. Kabeya, Y., Mizushima, N., Yamamoto, A., Oshitani-Okamoto, S., Ohsumi, Y., and Yoshimori, T. (2004). LC3, GABARAP and GATE16 localize to autophagosomal membrane depending on form-II formation. J. Cell Sci. *117*, 2805–2812. https://doi.org/10.1242/jcs.01131.

4. Ichimura, Y., Kirisako, T., Takao, T., Satomi, Y., Shimonishi, Y., Ishihara, N., Mizushima, N., Tanida, I., Kominami, E., Ohsumi, M., et al. (2000). A ubiquitin-like system mediates protein lipidation. Nature *408*, 488–492. https://doi.org/10.1038/35044114.

5. Kirisako, T., Ichimura, Y., Okada, H., Kabeya, Y., Mizushima, N., Yoshimori, T., Ohsumi, M., Takao, T., Noda, T., and Ohsumi, Y. (2000). The reversible modification regulates the membrane-binding state of Apg8/Aut7 essential for autophagy and the cytoplasm to vacuole targeting pathway. J. Cell Biol. *151*, 263–276. https://doi.org/10.1083/jcb.151.2.263.

6. Tanida, I., Sou, Y.s., Ezaki, J., Minematsu-Ikeguchi, N., Ueno, T., and Kominami, E. (2004). HsAtg4B/HsApg4B/autophagin-1 cleaves the carboxyl termini of three human Atg8 homologues and delipidates microtubule-associated protein light chain 3- and GABAA receptor-associated protein-phospholipid conjugates. J. Biol. Chem. *279*, 36268–36276. https://doi.org/10.1074/jbc.M401461200.

7. Agrotis, A., von Chamier, L., Oliver, H., Kiso, K., Singh, T., and Ketteler, R. (2019). Human ATG4 autophagy proteases counteract attachment

of ubiquitin-like LC3/GABARAP proteins to other cellular proteins. J. Biol. Chem. *294*, 12610–12621. https://doi.org/10.1074/jbc.AC119.009977.

8. Nguyen, T.N., Padman, B.S., Zellner, S., Khuu, G., Uoselis, L., Lam, W.K., Skulsuppaisarn, M., Lindblom, R.S.J., Watts, E.M., Behrends, C., and Lazarou, M. (2021). ATG4 family proteins drive phagophore growth independently of the LC3/GABARAP lipidation system. Mol. Cell *81*, 2013–2030.e9. https://doi.org/10.1016/j.molcel.2021.03.001.

9. Erard, M., Fredj, A., Pasquier, H., Beltolngar, D.-B., Bousmah, Y., Derrien, V., Vincent, P., and Merola, F. (2013). Minimum set of mutations needed to optimize cyan fluorescent proteins for live cell imaging. Mol. Biosyst. *9*, 258–267. https://doi.org/10.1039/C2MB25303H.

10. Bertolin, G., Sizaire, F., Déméautis, C., Chapuis, C., Mérola, F., Erard, M., and Tramier, M. (2019). Optimized FRET Pairs and Quantification Approaches To Detect the Activation of Aurora Kinase A at Mitosis. ACS Sens. *4*, 2018–2027. https://doi.org/10.1021/acssensors.9b00486.

11. Bousmah, Y., Valenta, H., Bertolin, G., Singh, U., Nicolas, V., Pasquier, H., Tramier, M., Merola, F., and Erard, M. (2021). tdLanYFP, a Yellow, Bright, Photostable, and pH-Insensitive Fluorescent Protein for Live-Cell Imaging and Förster Resonance Energy Transfer-Based Sensing Strategies. ACS Sens. *6*, 3940–3947. https://doi.org/10.1021/acssensors.1c00874.

12. Leray, A., Padilla-Parra, S., Roul, J., Héliot, L., and Tramier, M. (2013). Spatio-Temporal Quantification of FRET in living cells by fast time-domain FLIM: a comparative study of non-fitting methods [corrected]. PLoS One *8*, e69335. https://doi.org/10.1371/journal.pone.0069335.

13. Padilla-Parra, S., and Tramier, M. (2012). FRET microscopy in the living cell: different approaches, strengths and weaknesses. Bioessays *34*, 369–376. https://doi.org/10.1002/bies.201100086.

14. Bertolin, G., Marchand, G.L., and Tramier, M. (2020). Real-Time Monitoring of Aurora kinase A Activation using Conformational FRET Biosensors in Live Cells. JoVE, e61611. https://doi.org/10.3791/61611.

15. Cranfill, P.J., Sell, B.R., Baird, M.A., Allen, J.R., Lavagnino, Z., de Gruiter, H.M., Kremers, G.-J., Davidson, M.W., Ustione, A., and Piston, D.W. (2016). Quantitative assessment of fluorescent proteins. Nat. Methods *13*, 557–562. https://doi.org/10.1038/nmeth.3891.

16. Schindelin, J., Arganda-Carreras, I., Frise, E., Kaynig, V., Longair, M., Pietzsch, T., Preibisch, S., Rueden, C., Saalfeld, S., Schmid, B., et al. (2012). Fiji: an open-source platform for biological-image analysis. Nat. Methods *9*, 676–682. https://doi.org/10.1038/nmeth.2019.

17. Liu, P.-F., Tsai, K.-L., Hsu, C.-J., Tsai, W.-L., Cheng, J.-S., Chang, H.-W., Shiau, C.-W., Goan, Y.-G., Tseng, H.-H., Wu, C.-H., et al. (2018). Drug Repurposing Screening Identifies Tioconazole as an ATG4 Inhibitor that Suppresses Autophagy and Sensitizes Cancer Cells to Chemotherapy. Theranostics *8*, 830–845. https://doi.org/10.7150/thno.22012.

18. Akin, D., Wang, S.K., Habibzadegah-Tari, P., Law, B., Ostrov, D., Li, M., Yin, X.-M., Kim, J.-S., Horenstein, N., and Dunn, W.A. (2014). A novel ATG4B antagonist inhibits autophagy and has a negative impact on osteosarcoma tumors. Autophagy *10*, 2021–2035. https://doi.org/10.4161/auto.32229.

19. Berezin, M.Y., and Achilefu, S. (2010). Fluorescence Lifetime Measurements and Biological Imaging. Chem. Rev. *110*, 2641–2684. https://doi.org/10.1021/cr900343z.

20. Quinn, S.D., Dalgarno, P.A., Cameron, R.T., Hedley, G.J., Hacker, C., Lucocq, J.M., Baillie, G.S., Samuel, I.D.W., and Penedo, J.C. (2014). Real-time probing of β-amyloid self-assembly and inhibition using fluorescence self-quenching between neighbouring dyes. Mol. Biosyst. *10*, 34–44. https://doi.org/10.1039/c3mb70272c.

21. Chen, W., Young, L.J., Lu, M., Zaccone, A., Ströhl, F., Yu, N., Kaminski Schierle, G.S., and Kaminski, C.F. (2017). Fluorescence Self-Quenching from Reporter Dyes Informs on the Structural Properties of Amyloid Clusters Formed in Vitro and in Cells. Nano Lett. *17*, 143–149. https://doi.org/10.1021/acs.nanolett.6b03686.

22. Bae, W., Yoon, T.-Y., and Jeong, C. (2021). Direct evaluation of self-quenching behavior of fluorophores at high concentrations using an evanescent field. PLoS One *16*, e0247326. https://doi.org/10.1371/journal.pone.0247326.

23. Fu, Y., Hong, L., Xu, J., Zhong, G., Gu, Q., Gu, Q., Guan, Y., Zheng, X., Dai, Q., Luo, X., et al. (2019). Discovery of a small molecule targeting autophagy via ATG4B inhibition and cell death of colorectal cancer cells in vitro and in vivo. Autophagy *15*, 295–311. https://doi.org/10.1080/15548627.2018.1517073.

24. Redford, G.I., and Clegg, R.M. (2005). Polar Plot Representation for Frequency-Domain Analysis of Fluorescence Lifetimes. J. Fluoresc. *15*, 805–815. https://doi.org/10.1007/s10895-005-2990-8.